Multi-Phase Microstructure Control and Properties of 700MPa-Grade High-Strength High-Ductility Low-Carbon Low-Alloy Steel Postprint

Authors: Zhou Wenhao, Xie Zhenjia, Guo Hui, Shang Chengjia

Date: 2016-11-04T00:00:00+00:00

Abstract

This study investigated the microstructure evolution and mechanical properties of low-carbon low-alloy steel through a three-step continuous heat treatment process, namely intercritical annealing, intercritical tempering, and tempering. The results show that after intercritical annealing, the microstructure consisted of a dual-phase structure of lath-shaped intercritical ferrite and bainite; after intercritical tempering, it became a multi-phase structure comprising intercritical ferrite, tempered bainite, and retained austenite. The retained austenite exhibited granular and strip-like morphologies, distributed at ferrite/bainite phase interfaces and between bainite laths, with a content as high as 29%, and remained stable after tempering, primarily stabilized through the enrichment of C, Mn, Ni, and Cu in reversed austenite. During intercritical annealing and tempering, NbC precipitated in ferrite and bainite, showing spherical or irregular shapes with an average size of 10 nm; Cu-rich precipitates formed during intercritical tempering and tempering, spherically distributed in ferrite and retained austenite with sizes ranging from 10 to 30 nm. Through the strain-induced plasticity (TRIP effect) of retained austenite and the precipitation strengthening of nanoscale precipitates, the experimental steel exhibited excellent mechanical properties: yield strength higher than 700 MPa, tensile strength higher than 900 MPa, uniform elongation higher than 20%, and total elongation higher than 30%.

Full Text

The Regulation of Multi-Phase Microstructure and Mechanical Properties in a 700 MPa Grade Low Carbon Low Alloy Steel with Good Ductility

ZHOU Wenhao, XIE Zhenjia, GUO Hui, SHANG Chengjia
School of Materials Science and Engineering, University of Science and Technology Beijing, Beijing 100083

Correspondent: SHANG Chengjia, professor, Tel: (010) 62332428, E-mail: cjshang@ustb.edu.cn

Supported by National Basic Research Program of China (No.2010CB630081)

Manuscript received 2014-10-23, in revised form 2015-01-26

Abstract

Low carbon and low alloy steels require a good combination of strength and ductility to ensure the safety and stability of structures. Heat treatment in the intercritical region can produce multi-phase microstructure while simultaneously causing redistribution of alloying elements among different phases. Multi-step intercritical heat treatment is particularly favorable for obtaining retained austenite stabilized by repeated enrichment of alloying elements in reversed austenite, as well as nanometer-sized precipitates that primarily form during tempering. The excellent mechanical properties arise from the combined effects of transformation-induced-plasticity (TRIP) from retained austenite and precipitation hardening from nanometer-sized precipitates.

This paper investigates the microstructural evolution and corresponding mechanical properties of a low carbon low alloy steel processed by a three-step heat treatment: intercritical annealing, intercritical tempering, and final tempering. After intercritical annealing, the microstructure consisted of a typical dual-phase structure of intercritical ferrite and bainite/martensite. Following intercritical tempering, the microstructure primarily comprised intercritical ferrite, tempered bainite/martensite, and retained austenite. Retained austenite with a volume fraction of 29% was distributed at ferrite/bainite (martensite) boundaries and between bainitic/martensitic laths. This retained austenite was stabilized by enrichment of C, Mn, Ni, and Cu in the reversed austenite during the reversion transformation process. NbC precipitates with an average size of 10 nm formed in the ferrite matrix and bainite/martensite, while Cu-containing particles in the size range of 10-30 nm precipitated in ferrite and retained austenite during intercritical tempering and tempering. The morphology of NbC precipitates was spherical, elliptical, and irregular, while copper precipitates were spherical. Through the combined effects of transformation-induced-plasticity (TRIP) from retained austenite and precipitation hardening, the steel achieved

outstanding mechanical properties: yield strength > 700 MPa, tensile strength > 900 MPa, uniform elongation > 20%, and total elongation > 30%.

KEY WORDS high performance, intercritical heat treatment, multi-phase microstructure, retained austenite, nanometer-sized precipitate

---

Introduction

Low alloy steels are widely used in construction facilities and energy industries. To ensure structural reliability and safety, these materials require high strength and high toughness/plasticity. With rapid industrial development and increasing environmental awareness, demands for lightweight engineering structures and equipment are growing, which urgently requires higher strength in steel materials. While single strengthening mechanisms and methods are well understood—through thermomechanical processing and heat treatment, steel strength can easily reach the GPa level—such simple strength enhancement typically leads to reduced toughness and plasticity. For steel materials, only when strength is increased while continuously absorbing energy during deformation and fracture does the enhancement become meaningful [1].

Retained austenite can trigger the transformation-induced plasticity (TRIP) effect during deformation, transforming into martensite, absorbing deformation energy, and delaying necking, thereby achieving simultaneous improvement of strength and plasticity. Therefore, introducing retained austenite into steel is an effective approach to obtain a good strength-ductility balance. How to obtain sufficient and stable retained austenite has been a research hotspot in recent years. One method is to modify the steel' s chemical composition design by increasing the content of austenite-stabilizing elements to obtain austenite structure, such as in high-Ni austenitic stainless steels [2,3] and high-Mn twinning-induced plasticity (TWIP) steels [4,5]. However, due to excessively high alloy element content, this method increases steel costs while also creating difficulties in the smelting process. Another method is to obtain stable retained austenite through heat treatment, commonly using TRIP [6,7] and quenching & partitioning (Q&P) processing [8,9]. During such heat treatment processes, C atoms diffuse from bainite or martensite into untransformed austenite for enrichment, significantly improving the stability of untransformed austenite and thus obtaining retained austenite stable at room temperature. Since retained austenite is obtained through C atom enrichment, the C content in such steels is typically higher than 0.2% (mass fraction). This is undesirable for structural materials because high C content greatly reduces steel' s weldability. Therefore, under the premise of low C and low alloy, improving performance by obtaining retained austenite simultaneously ensures good weldability and low cost, which is of great significance for developing high-strength steels.

In steels with precursor microstructures of lath martensite or bainite, when heated to the $\alpha+\gamma$ two-phase region, reverse-transformed austenite nucleates

and grows between laths. This austenite appears needle-like or lath-shaped and is enriched with alloying elements. As the isothermal temperature in the two-phase region increases and holding time extends, austenite transforms toward granular morphology, and the enriched alloying elements gradually decrease [10]. At lower two-phase region temperatures, the C content in austenite is higher, making austenite more stable. Therefore, stable austenite structure can be obtained through reasonable control of temperature and time in the two-phase region.

As early as the 1970s, Miller [11] and Niikura et al. [12] obtained retained austenite in high-Ni steels through intercritical annealing treatment. Due to high Ni content, a large amount of retained austenite could be obtained with just one-step intercritical treatment. As annealing time extended, the Ni content enriched in reversed austenite increased, yielding more retained austenite at room temperature. In recent years, Luo et al. [13] and Shi et al. [14] proposed the austenite reversion transformation (ART) theory, achieving retained austenite content as high as 40% in 0.2C-5Mn steel after intercritical annealing treatment. Combined with ultrafine-grained ferrite matrix, excellent strength-ductility matching can be obtained. For low-Ni steels, because Ni enrichment during one-step intercritical treatment is insufficient to stabilize reversed austenite to room temperature, two-step or even multi-step continuous intercritical processing is needed. In such multi-step intercritical heat treatment processes, the intercritical treatment temperature gradually decreases because element enrichment from the previous step reduces the phase transformation point in that region [15]. Residual austenite obtained through this multi-step intercritical treatment has high alloy content, fine size, and high stability. This provides a new approach for obtaining retained austenite in low alloy systems: through continuous intercritical heat treatment to enable multiple enrichments of alloying elements in reversed austenite, stabilizing reversed austenite to obtain retained austenite.

This work investigates a low C, Nb-Cu microalloyed low alloy steel using multi-step intercritical processing to study the relationship between microstructure and properties during different heat treatments. Combining optical microscopy, scanning electron microscopy, electron backscatter diffraction and transmission electron microscopy, the microstructure was characterized, focusing on revealing the variation patterns of retained austenite and nanoscale precipitates. Simultaneously, combined with mechanical property curves, the effects of retained austenite and precipitates on properties were investigated. This study aims to understand the microstructural evolution mechanisms in low alloy steel during continuous intercritical processing, providing theoretical basis for technical solutions such as microstructure control and performance optimization of high-performance low alloy steels.

Experimental

The chemical composition of the experimental 700 MPa grade high-strength high-ductility steel (mass fraction, %) was: C 0.10, Mn 2.01, Si 0.78, Al 0.78, Nb 0.078, Cu 1.0, Ni 1.0, Mo 0.26, Fe balance. To ensure weldability, low C design was adopted. Mn and Ni are austenite-stabilizing elements, Nb, Cu and Mo are precipitation-strengthening elements, and Si and Al prevent cementite formation, ensuring more C atoms can participate in the process of stabilizing austenite and forming precipitates. The experimental steel was smelted using a 50 kg vacuum induction furnace, then rolled into 8 mm thick plates and air-cooled to room temperature. Tensile heat treatment specimens with dimensions of 10 mm × 8 mm × 90 mm were taken along the rolling direction, and after heat treatment were processed into standard round-bar tensile specimens with a diameter of 5 mm (gauge length 25 mm). Phase transformation points were measured using the dilatometric method according to YB/T 5127-93 with a heating rate of 0.05 °C/s.

Dilatometric measurement showed that for the experimental steel in equilibrium, the starting temperature of ferrite-to-austenite transformation (Ac1) and the temperature at which ferrite completely transforms to austenite (Ac3) were 660 °C and 928 °C, respectively. The heat treatment process was: specimens were heated to the two-phase region at 780 °C, held for 30 min, then air-cooled to room temperature; subsequently reheated to the two-phase region at 660 °C, held for 30 min, then air-cooled to room temperature; finally reheated to 500 °C, held for 30 min, then air-cooled to room temperature (Figure 1 [FIGURE:1]). The selection of heat treatment temperatures is described in references [15, 16]. In this study, samples after one-step, two-step and three-step heat treatments were designated as samples A, B and C, respectively. Specimens were cut from the undeformed ends of fractured tensile samples, ground and polished, etched with LePera reagent, and observed under a BX51M optical microscope (OM). Microstructures were also observed under an Ultra 55 field emission scanning electron microscope (SEM) after etching with 3% nital. Electron backscatter diffraction (EBSD) analysis was performed after electropolishing using a solution of HClO4:C3H8O3:C6H2O = 0.5:1:8.5 (volume ratio) at 20 kV acceleration voltage, 15 mm working distance, 70° tilt angle, and 0.08 m scan step. Retained austenite in the experimental steel was measured using a DMAX-RBX X-ray diffractometer (XRD) with the five-peak method according to GB8362-87. Samples 0.4 mm thick were taken from both ends of tensile bars, ground to 100 m thickness, then punched into 3 mm diameter discs and further ground to 50-60 m thickness before twin-jet thinning. The twin-jet solution was 5% perchloric acid alcohol solution at -20 °C. Microstructure and precipitate observations were conducted using a JEM-2100F transmission electron microscope (TEM) equipped with an energy dispersive spectrometer (EDS) at 200 kV operating voltage.

2.1 Microstructure and Mechanical Properties

Figure 2 [FIGURE:2] shows the phase transformation points of the experimental steel at different heat treatment stages measured by dilatometry. After hot rolling, the starting temperature of bcc-to-fcc transformation (Ac1) in equilibrium was 660 °C, which decreased to 641 °C after the first-step treatment, and further decreased to 607 °C after the second-step tempering. This indicates that the reverse transformation from bcc to fcc phase can proceed during the second-step heat treatment at 660 °C. The reason for the Ac1 temperature decrease is the redistribution of alloying elements during intercritical heat treatment; enrichment of alloying elements in reversed austenite lowers the phase transformation temperature in that region. The decrease in Ac1 temperature not only enables the next intercritical heat treatment to be conducted at lower temperature but also facilitates the formation of finer precipitates.

Figures 3 [FIGURE:3] and 4 [FIGURE:4] show OM and SEM images of the experimental steel after different heat treatment stages, respectively. Before heat treatment, the specimen primarily consisted of lath bainite/martensite microstructure (Figures 3a and 4a). The microstructure continuously evolved with changes in intercritical treatment temperature and steps. After intercritical annealing at 780 °C, the microstructure mainly consisted of a dual-phase structure of ferrite and bainite/martensite, with ferrite distributed as irregular blocky or lath shapes between bainite/martensite laths (Figures 3b and 4b). After intercritical tempering at 660 °C, ferrite showed no obvious change, but the content of bainite/martensite in the microstructure decreased. SEM images revealed that bainite/martensite decomposed into fine granular structures distributed dispersedly around ferrite grains (Figure 4c). Comparing with OM images (Figure 3c), these granular structures were primarily retained austenite. This demonstrates that during intercritical tempering, bainite/martensite transformed into retained austenite through reverse transformation. The average diameter of retained austenite particles was below 1 m. After tempering at 500 °C, the microstructure showed no obvious change, still primarily consisting of ferrite and retained austenite, while the content of bainite/martensite significantly decreased after two tempering steps (Figures 3d and 4d).

The mechanical properties of the experimental steel at different heat treatment stages are shown in Table 1 . After intercritical annealing, the yield strength was 686 MPa and tensile strength reached 1178 MPa, but elongation was low with uniform elongation of only 6.3% and total elongation of 17%. After the second-step intercritical tempering, yield strength increased to 707 MPa, tensile strength decreased to 845 MPa, and elongation significantly increased, with uniform elongation and total elongation exceeding 20% and 30%, respectively, and the product of strength and ductility approaching 30 GPa · %. After the third-step tempering, yield strength increased by 17 MPa and tensile strength increased by 78 MPa, while uniform and total elongation showed no significant decrease.

2.2 Retained Austenite

Figure 5 [FIGURE:5] shows EBSD characterization of retained austenite distribution and XRD spectra of the experimental steel at various heat treatment stages. Black lines represent low-angle grain boundaries with misorientation less than 10°, and red regions represent retained austenite. As seen in Figures 5a-c, retained austenite was primarily distributed at grain boundaries. XRD spectral calculations showed that retained austenite content was low after intercritical annealing, only about 5%. After the second-step intercritical tempering treatment, retained austenite content reached as high as 29%, and after the third-step tempering, retained austenite content did not decrease. This indicates that retained austenite obtained through two-step intercritical treatment has high thermal stability. TEM images (Figure 6 [FIGURE:6]) revealed that retained austenite appeared as lath or granular shapes distributed at ferrite grain boundaries or ferrite/bainite phase interfaces. No retained austenite was observed inside ferrite grains. EDS analysis showed that the average Mn and Ni contents in retained austenite were much higher than in the ferrite matrix (Figure 6a), consistent with Xie et al.' s research results [17]. This suggests that alloying elements diffused and enriched from ferrite and bainite/martensite into critical austenite during intercritical processing. Therefore, it is necessary to investigate the partitioning behavior of alloying elements in different phases during intercritical treatment.

Thermal-Calc was used to calculate the equilibrium distribution of alloying elements in austenite and ferrite after intercritical annealing at 780 °C for 30 min, as shown in Table 2 . At equilibrium at 780 °C, the volume fractions of ferrite and austenite were 55% and 45%, respectively. Austenite-stabilizing elements C, Mn, Ni and Cu were all enriched to some extent in austenite. The martensite start temperature (Ms) of this austenite portion was 333 °C, indicating that the enrichment degree of alloying elements at this temperature was insufficient to stabilize austenite to room temperature. During cooling, austenite transformed into bainite/martensite structure, consistent with microstructural observations. SEM observation showed that during the second-step intercritical treatment, mainly bainite/martensite microstructure changed. Therefore, studying the phase transformation behavior of this microstructure portion at 660 °C was necessary. Table 2 also shows the distribution of alloying elements in the microstructure at 660 °C for this alloy composition system. According to Thermal-Calc calculations, the precipitation temperature of Cu during cooling was 680 °C, indicating that Cu precipitates formed during isothermal holding at 660 °C. After reverse transformation at 660 °C, alloying elements further enriched in the newly formed austenite, with C content of 0.5%, Mn content as high as 6.1%, and certain enrichment of Cu and Ni. The Ms of this austenite portion was 120 °C, suggesting that austenite would still transform to martensite during cooling. However, after actual two-step treatment, retained

austenite content obtained at room temperature reached as high as 29%. This is because, in addition to chemical composition, the size of retained austenite is also a key factor affecting its stability. Takaki et al. [18] demonstrated that smaller retained austenite size leads to lower Ms and higher stability. When retained austenite grain size is less than 1 m, martensite nucleation within austenite requires extremely large chemical driving force, thus effectively preventing austenite-to-martensite transformation. Therefore, retained austenite stability results from the combined effects of alloying element enrichment and grain size.

Alloy element diffusion is determined by both temperature and diffusion time. In two-dimensional space, diffusion distance is determined by the diffusion coefficient and diffusion time of alloying elements. Table 3 lists the diffusion distances of C, Mn, Ni and Cu elements at different temperatures. The calculation results show that C' s diffusion coefficient and distance in ferrite are several orders of magnitude higher than other elements. At 660 °C, the diffusion distances of Mn, Ni and Cu were 212, 95 and 120 nm, respectively. At 500 °C, except for C which still had relatively high diffusion ability, diffusion of other elements could be neglected. Comparing with ferrite and bainite/martensite grain sizes in SEM images, alloy element diffusion mainly occurred during the first two intercritical treatment steps.

The C content of retained austenite obtained through the two-step method was 0.5%, which is much lower than that in conventional TRIP steel retained austenite (1.1%~1.7%) [19]. EDS measurement showed Mn content in retained austenite as high as 5.0% and Ni content reaching 1.6%. This indicates that retained austenite obtained through the two-step method was primarily stabilized through enrichment of Mn and Ni.

In TRIP or Q&P steels, C atoms enrich from bainite or martensite laths into adjacent austenite during isothermal quenching or partitioning, thereby obtaining retained austenite stable at room temperature. This type of austenite forms at medium-low temperature isothermal stages and has high C content. During high-temperature tempering stages, it decomposes into cementite and ferrite [20]. However, as the Mn and Ni contents in retained austenite increase, its tempering stability increases. During multi-step intercritical heat treatment, retained austenite stability is primarily improved through enrichment of alloying elements such as Mn and Ni in reversed austenite, with very low C content, which greatly reduces the chemical driving force for cementite formation during tempering. Meanwhile, the high Si and Al contents in the experimental steel effectively inhibit cementite formation. Therefore, after tempering, no cementite structure was observed in the microstructure, and retained austenite could still maintain high content.

2.3 Nanometer-Sized Precipitates

Forming precipitates by adding microalloying elements to steel is a conventional method for improving steel strength. Nb and Cu, as common precipitate-forming elements, have equilibrium precipitation start temperatures of 1200 °C and 680 °C, respectively (Thermal-Calc calculation). This indicates that Nb begins to precipitate during hot rolling, while Cu precipitates can only form at lower temperatures. To investigate the precipitation behavior of Nb and Cu at different heat treatment stages, carbon replica and thin foil specimens were observed by TEM, and precipitate sizes were statistically analyzed. Figure 7 [FIGURE:7] shows TEM images of carbon replica-extracted precipitates in the experimental steel after hot rolling, intercritical annealing and intercritical tempering. As seen, after hot rolling, two types of precipitates with different sizes were observed: one type larger than 20 nm with irregular shape, formed at relatively high temperatures and contributing little to strength; the other type between 4-14 nm, spherical and distributed in the matrix (Figure 7a), formed during rolling or cooling processes. The average precipitate size was 10.9 nm (Figure 7b), and EDS results indicated these precipitates were NbC. After intercritical annealing, most newly formed NbC precipitates concentrated in the 7-15 nm range, spherical and dispersedly distributed in the matrix (Figures 7c and d). After intercritical tempering, the average NbC size decreased to about 6.0 nm because numerous fine precipitates (3-8 nm) formed at this stage (Figures 7e and f). After intercritical tempering, in addition to fine NbC precipitates, numerous Cu precipitates were also observed in the ferrite matrix (Figure 8a [FIGURE:8]). Cu precipitate particle sizes distributed between 10-30 nm (Figure 8b), spherical or ellipsoidal and distributed in ferrite. Considering the influence of Nb precipitates, particles below 10 nm were ignored when statistically analyzing Cu precipitate sizes. These results indicate that Nb began to precipitate during hot rolling and continued to precipitate during intercritical annealing and tempering, with precipitate size decreasing as temperature decreased. Cu precipitated during intercritical tempering, with relatively large precipitate particle sizes.

After the third-step tempering treatment, numerous precipitate particles appeared in retained austenite (Figures 8c-e). EDS analysis identified them as Cu precipitates (Figure 8f). Precipitate sizes were between 10-20 nm. Cu precipitation was also observed in adjacent ferrite, but with much lower density than in austenite. Cu precipitate distribution in ferrite was non-uniform, with higher Cu precipitate density in ferrite adjacent to retained austenite and lower density in large ferrite regions far from austenite (Figure 7c). This also indicates that Cu element redistribution occurred during the first two heat treatment steps, i.e., diffusion enrichment from ferrite into austenite. Generally, due to Cu' s high solubility in austenite, it is difficult to precipitate in austenite. Chi et al. [21] studied Cu-containing austenitic stainless steels and showed that Cu precipitation in austenite proceeds through diffusion to form Cu-rich regions in local areas of austenite, followed by gradual precipitation during aging. This requires

not only high Cu content (mass fraction >2%) but also long isothermal time (>5h) to form Cu precipitates in austenite. In this experiment, Cu enrichment in reversed austenite during intercritical annealing and tempering prepared the formation of Cu-rich regions; moreover, Cu precipitation was relatively active at 500 °C, so Cu precipitated in austenite after the third-step tempering treatment.

During intercritical treatment, enrichment of alloying elements in reversed austenite not only improved austenite stability but also lowered the equilibrium bcc-to-fcc transformation start temperature Ac1, as shown in Figure 2 [FIGURE:2]. The decrease in Ac1 enabled the next intercritical treatment to be conducted at lower temperature and facilitated the formation of smaller precipitates at low temperature, thereby ensuring that large amounts of retained austenite and Nb and Cu precipitates could be obtained simultaneously during intercritical tempering. After two-step heat treatment, ferrite content was about 50% [16], comparable to conventional C-Mn-Si TRIP steel [22], but with higher strength and plasticity than traditional TRIP steel (yield strength 400-600 MPa, total elongation 20%-30%) [23].

This is related to the ultrafine microstructure, stable retained austenite and nanoscale precipitates in the experimental steel. Unlike the bulky polygonal ferrite in TRIP steel, ferrite obtained in the intercritical region appeared as fine lath or block shapes distributed between bainite/martensite laths, retaining numerous dislocations inside. This ultrafine ferrite microstructure also appears in Q&P steels and medium-Mn steels processed by austenite reversion transformation (ART), and is considered one of the factors causing high yield strength. Nanoscale precipitates formed during tempering were dispersedly distributed in ferrite, greatly strengthening the ferrite matrix. Studies by Funakawa et al. [24] and Yen et al. [25] showed that when precipitate size in ferrite is below 5 nm, the contribution of precipitation to yield strength exceeds 300 MPa. Therefore, despite high ferrite content, the experimental steel still possessed very high yield strength.

After the third-step tempering treatment, Cu continued to precipitate in ferrite and austenite. However, due to relatively large Cu precipitate particle sizes, the contribution to yield strength was not significant. Compared with the second-step intercritical tempering, yield strength increased by 17 MPa, but tensile strength increased substantially. This is related to Cu precipitation in retained austenite. On one hand, enrichment of alloying elements and precipitation in austenite increased austenite strength [26], increasing the proportion of hard phases in the microstructure. On the other hand, retained austenite absorbs dislocations from surrounding microstructure during deformation, leading to increased dislocation density inside austenite [27]. Interaction between Cu precipitates and dislocations also strengthened austenite and improved its stability to some extent. Additionally, after austenite transformed to martensite during deformation, Cu precipitation also strengthened martensite. After tempering treatment, the work hardening rate of the experimental steel was significantly improved [28], ensuring high tensile strength while maintaining high

yield strength.

Conclusions

1. Intercritical heat treatment causes enrichment of alloying elements in reversed austenite, thereby lowering the phase transformation point of reversed microstructure and enabling the next reverse transformation to occur at lower temperature. Continuous intercritical treatment allows this reverse transformation to proceed repeatedly, improving austenite stability through multiple enrichments of alloying elements in reversed austenite to obtain retained austenite stable at room temperature. Meanwhile, the gradually decreasing intercritical treatment temperature reduces precipitate size and promotes formation of low-temperature precipitates, enabling simultaneous acquisition of retained austenite and precipitates in the same processing step and effectively combining precipitation strengthening with the TRIP effect of retained austenite. Through multi-phase microstructure, TRIP effect and precipitation strengthening, the low carbon low alloy experimental steel possesses excellent mechanical properties: yield strength $>$ 700 MPa, tensile strength $>$ 900 MPa, uniform elongation and total elongation $>$ 20% and 30%, respectively.

2. After continuous three-step heat treatment of intercritical annealing, intercritical tempering and tempering, a multi-phase microstructure was obtained consisting of lath ferrite matrix, lath bainite/martensite and retained austenite. Retained austenite had average size less than 1 m, distributed at ferrite/bainite (martensite) phase boundaries and bainite/martensite lath boundaries. Retained austenite primarily formed during intercritical tempering, stabilized mainly by enrichment of C, Mn, Ni and Cu in reversed austenite, with content as high as 29%. High alloy element content and fine size gave retained austenite high stability. During the third-step tempering process, retained austenite remained stable with unchanged content.

3. The microstructure mainly contained two types of precipitates: NbC and Cu. The former precipitated during all three heat treatment steps, with size gradually decreasing as temperature decreased, dispersedly distributed in ferrite and bainite/martensite. The latter partially precipitated in ferrite during intercritical tempering, and mainly precipitated in ferrite and retained austenite during tempering. NbC precipitation prevented strength loss during high-temperature annealing and tempering, ensuring high strength of the matrix microstructure. In addition to precipitation strengthening, Cu precipitation in retained austenite improved austenite stability to some extent, thereby increasing work hardening rate and tensile strength.

References

[1] Dong H, Wang M Q, Weng Y Q. Iron Steel, 2010; 45 (7): 3 (董瀚, 王毛球, 翁宇庆. 钢铁, 2010; 45: 3)
[2] Liu L, Yang Z G, Zhang C, Liu W B. Mater Sci Eng, 2010; A527: 7205
[3] Yoo J D, Hwang S W, Park K T. Mater Sci Eng, 2009; A508: 234
[4] Misra R D K, Challa V S A, Venkatsurya P K C, Shen Y F, Somani M C, Karjalainen L P. Acta Mater, 2015; 84: 339
[5] Lee T, Koyama M, Tsuzaki K, Lee Y H, Lee C S. Mater Lett, 2012; 75: 169
[6] Sugimoto K I, Mobayashi M, Hashimoto S I. Metall Mater Trans, 1992; 23A: 3085
[7] Sugimoto K I, Tsunezawa M, Hojo T, Ikeda S. ISIJ Int, 2004; 44: 1608
[8] Speer J G, Matlock D K, De Cooman B C, Schroth J G. Acta Mater, 2003; 51: 2611
[9] Misra R D K, Zheng H, Wu K M, Karjalainen L P. Mater Sci Eng, 2013; 579A: 188
[10] Kang J, Zhou X G, Wang G D. Steel Rolling, 2009; 26 (3): 34 (康健, 周晓光, 王国栋. 轧钢, 2009; 26: 34)
[11] Miller R L. Metall Trans, 1972; 3: 905
[12] Niikura M, Morris J W. Metall Trans, 1980; 11: 1531
[13] Luo H W, Shi J, Wang C, Cao W Q, Sun X J, Dong H. Acta Mater, 2011; 59: 4002
[14] Shi J, Sun X J, Wang M Q, Hui W J, Dong H, Cao W Q. Scr Mater, 2010; 63: 815
[15] Zhou W H, Guo H, Xie Z J, Wang X M, Shang C J. Mater Sci Eng, 2013; A587: 366
[16] Zhou W H, Wang X L, Venkatsurya P K C, Guo H, Shang C J, Misra R D K. Mater Sci Eng, 2014; A607: 569
[17] Xie Z J, Yuan S F, Zhou W H, Yang J R, Guo H, Shang C J. Mater Des, 2014; 59: 195
[18] Takaki S, Fukunaga K, Syarif J, Tsuchiyama T. Metall Trans, 2004; 45: 2251
[19] Sakuma Y, Matsumura O, Takechi H. Metall Trans, 1991; 22A: 489
[20] Thomas G. Metall Trans, 1978; 9A: 447
[21] Chi C Y, Dong J X, Liu W Q, Xie X S. Acta Metall Sin, 2010; 46: 1145 (迟成宇, 董建新, 刘文庆, 谢锡善. 金属学报, 2010; 46: 1145)
[22] Ray A, Dhua S K. Mater Charact, 1996; 37: 1
[23] Zhang Y H, Zhao H J, Kang Y L. Hot Working Tech, 2006; 35 (6): 62 (张迎晖, 赵鸿金, 康永林. 热加工工艺, 2006; 35 (6): 62)
[24] Funakawa Y, Shiozaki T, Tomita K, Yamamoto T, Maeda E. ISIJ Int, 2004; 44: 1945
[25] Yen H Y, Chen P Y, Huang C Y, Yang J R. Acta Mater, 2011; 59: 6264
[26] He B B, Huang M X, Liang Z Y, Ngan A H W, Luo H W, Shi J, Cao W Q, Dong H. Scr Mater, 2013; 69: 216
[27] Zhang K, Zhang M H, Guo Z H, Chen N L, Rong Y H. Mater Sci Eng, 2011; 528A: 8486

[28] Zhou W H, Guo H, Xie Z J, Shang C J. Mater Des, 2014; 59: 195

Figures

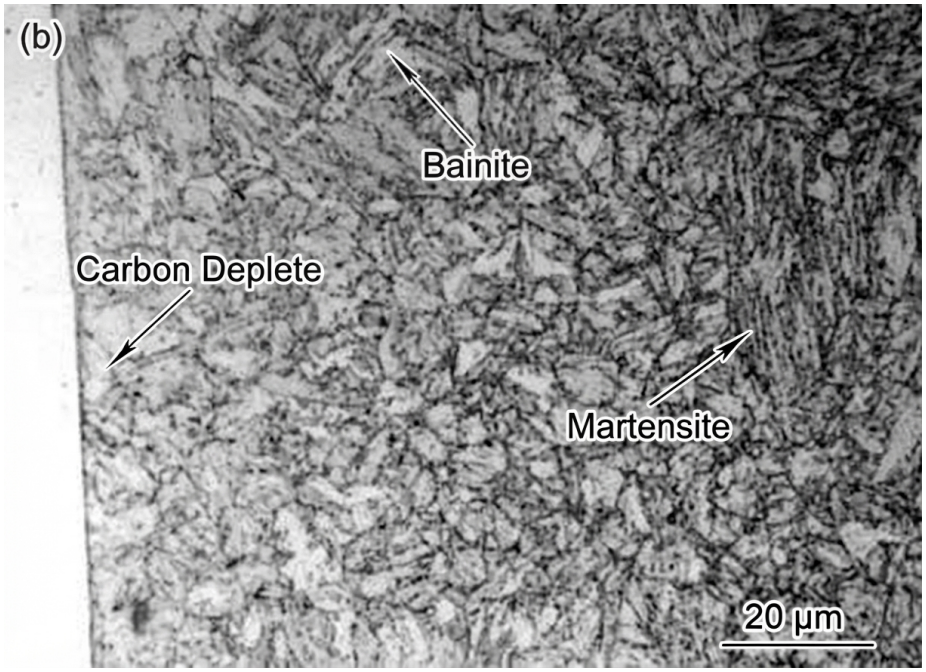

Figure 1: Figure 14